J. Webster (ed.), *Wiley Encyclopedia of Electrical and Electronics Engineering*

MAGNETIC THIN FILMS

Magnetic thin films are increasingly utilized for sensors/devices (for example, see related entries on Magnetic Bubble Memory, Magnetic Microwave Devices, Magnetic Recording Heads, Magnetic Sensors, Magnetic Storage Media, Magnetic Tapes, Magnetoresistance, and Magnetostrictive Devices. They are also increasingly important test structures for fundamental studies of magnetism (for example, see related entries on Magnetic Epitaxial Layers, and Magnetic Semiconductors. Depending on the application or purpose, magnetic thin films can be composed of single layer or multilayer materials. In addition, they can be fabricated in a variety of crystalline and chemical forms (for example: elements, alloys, oxides, nitrides, and intermetallics). Magnetic films are fabricated to enhance specific properties including saturation magnetization, anisotropy, magneto-optic activity, conduction electron spin polarization, exchange coupling, coercivity, conductivity, remanence, squareness and energy product. These properties are all intimately coupled with the choice of film materials and the detailed nature of the thin film fabrication process (and its connection with film microstructure). Consequently, the development of new magnetic thin film materials and processes is a major focus of academic and industrial research and development activity.

Research in magnetic film materials has progressed enormously since Bruck's pioneering demonstration of the epitaxial growth of iron films on NaCl in the 1930s (1). Since the 1980s, magnetic film research has been spurred by rapidly changing technological, computational, and economic factors (2,3,4,5,6,7,8,9,10,11). One factor is the advent of new and/or improved film fabrication techniques (molecular beam epitaxy, ultrahigh vacuum evaporation, variant sputtering techniques, chemical vapor deposition, pulsed laser deposition or ablation, electrodeposition, spin–spray methods, liquid phase epitaxy, etc.) utilizing rapidly evolving improvements in vacuum technology, deposition sources, and source materials that permit the fabrication of increasingly precise artificial magnetic film structures with potentially monolayer thickness control. These technological improvements related to film processing have permitted the fabrication of new, artificially structured magnetic thin films that exhibit new and interesting properties that compare more directly with fundamental theoretical models, and raise the possibility of industrially fabricated magnetic film sensors and devices with useful, reliable performance and yield (12,13,14). It should be noted that there is no single universally superior magnetic film fabrication process, and that these various film processing methods often have complementary advantages for niche applications.

A second key technological factor is the availability of improved and sophisticated magnetic film (4), general thin film (15), and general surface science characterization techniques (16) available for use in small laboratory settings and/or centrally located laboratory settings (such as at national laboratories). A third key factor is the increasing availability of fast, inexpensive, and numerically intensive computers appropriate for use with advanced new computational algorithms focused towards the solution of magnetic film system models with subtle quantum mechanical effects in complicated geometries typically encountered in fundamental and device experimental systems (17). A final key factor arousing the keen modern interest in magnetic films is the lucrative economic incentive for developing new magnetic film materials suitable for faster and higher density information storage systems with improved reliability and signal-to-noise characteristics to meet the highly competitive demands for information storage. For perspective on the rapid growth of this industrial demand,

consider that the world-wide magnetics industry has grown from a "several billion dollar" industry in the early 1980s (18) to an estimated $60 billion industry in 1992 (19). Furthermore, revenues from the rigid disk drive segment, which represents the largest industrial demand for magnetic thin materials, is forecast to surge from $29.6 billion in 1996 to $38.7 billion in 2001 (19, 20). There is also emerging interest in magnetic film materials for use in hybrid magnet–semiconductor structures and magnetoelectronic devices such as magnetic random access memories and spin transistors (11, 21, 22).

In this article, we will briefly survey the basic concepts of thin film formation appropriate for magnetic thin films. Next, we will briefly discuss the most popular basic types of film fabrication methods for producing most varieties of magnetic film structures. Lastly, we will review important examples of how the choice of thin film fabrication process, substrate, and processing parameters can be used to control the microstructure and resultant properties of magnetic thin films used for both fundamental and applied research. We will also briefly survey the important classes of magnetic film structures that are of current interest to the magnetic film community.

Basic Concepts for Magnetic Thin Film Formation

There are various new or improved methods for fabricating magnetic thin film materials, which will be briefly reviewed in the next section. Regardless of the method used for generating flux material for fabricating magnetic thin films, the arriving flux material can form various types of magnetic film structures depending on the conditions present when the flux encounters the substrate, or the conditions present after film growth (i.e., postgrowth annealing). Since magnetic film properties (saturation magnetization, anisotropy, magnetostriction, etc.) correlate with magnetic film microstructure, magnetic film materials can be artificially engineered for use in fundamental investigations of magnetism or for implementation in new magnetic devices. Although the understanding of thin film formation is incomplete, there is a framework available for describing it that is sufficiently useful for guiding attempts towards developing artificially engineered magnetic films. This framework is outlined in detail in recent reviews (23, 24), and is summarized in this section. Since single-crystalline, textured, polycrystalline, and amorphous magnetic films hold considerable interest for various segments of the magnetic film community, we review basic concepts by which these types of magnetic films can be fabricated.

Adsorption and Initial Nucleation. Substrate materials with amorphous, polycrystalline, and single-crystalline surfaces are commonly used for fabricating magnetic films. The flux of atoms or molecules that impinge on the substrate will first adsorb on the substrate surface, then typically will diffuse some distance across the surface before becoming incorporated into the film. This surface diffusion is often limited by the arrival of subsequent flux material. Film incorporation involves the reaction of the adsorbed species with each other and the surface to form the bonds of the film material. The initial aggregation of the incorporated species on the substrate surface is called *nucleation*. The evolution of the film structure after nucleation determines properties such as its crystallinity and morphology (e.g., roughness or columnarity).

Generally, the flux species will feel a weak van der Waals (dipolar) attraction (typically $E_d < 0.25$ eV) to the surface atomsr molecules when they are brought within a few atomic distances of the surface. The attraction will be stronger if the molecules involved are polar, resulting in a deeper potential well, which more efficiently traps or accommodates the flux species on the substrate surface. The atoms trapped in the dipolar van der Waals potential wells are described as *physisorbed*.

The accommodated physisorbed atoms or molecules can then migrate across the substrate surface atomic sites, occasionally gaining enough thermal energy fluctuations from the substrate to desorb. If they can form chemical bonds with the surface atoms, the surface-diffusing physisorbed species fall into a deeper (more attractive) chemisorption potential well (0.3 eV $< E_r <$ 10 eV). If chemisorption states are available, the physisorbed states are called *precursor* states. There is an activation energy between precursor and chemisorbed

states that results in a chemisorption reaction rate that competes with the probability for precursor reevaporation from the surface. Generally, there is a substrate temperature range, or *window,* for promoting surface diffusion and chemisorption processes during film growth that exceeds the loss of material at the surface due to reevaporation.

Uncontrolled impurities (such as adsorbed water) on the surface of a substrate often lead to especially weak van der Waals attractions and often suppress desired chemisorption processes, resulting in magnetic films with poor adhesion and often irregular properties among otherwise identical samples. This is especially well chronicled in older reviews of metallic magnetic films on air-cleaved and vacuum-cleaved alkali halide substrates (25, 26), where limitations in film fabrication technology and materials led to nearly uncontrollable substrate surface conditions that produced films with greatly divergent properties that created considerable controversy among researchers. On the other hand, magnetic film growth can often be improved by the presence of certain seed or buffer layers, which establish desirable chemisorption states and promote desired film structure. We will survey a few important examples of this seeding strategy for magnetic film materials later in this review.

Absolute reaction rate theory provides us with a qualitative insight into the nature of surface diffusion processes (24). If the desorption activation energies for physisorption (dipolar) sites and chemisorption sites are given as E_d and E_c, respectively, then there are also smaller potential barrier variations (the surface diffusion activation energy E_s is always considerably less than $E_d \ll E_c$) along the surface in between surface atom sites, resulting in additional surface diffusion adsorption sites. These barriers represent corrugation adsorption sites for surface diffusion involving the partial breaking of bonds between the adsorbate and the surface diffusion sites. The application of statistical mechanics to this model results in an insightful relation describing the rate of surface diffusion barrier crossing by transition state molecules per unit area of surface (R_s):

$$R_s = n_s \left(\frac{k_B T}{h}\right) \quad \exp\left(\frac{-E_s}{RT}\right) = n_s k_s \qquad (1)$$

in terms of the concentration of atoms/molecules in the surface diffusion adsorption sites (n_s), the universal gas constant (R), the Boltzmann constant (k_B), Planck's constant (h), the surface diffusion activation energy (E_s), and the temperature (T). Note that the rate constant for surface diffusion (k_s) represents the frequency with which an individual adsorbate atom or molecule hops to an adjacent site, and that the exponential prefactor $k_B\, T\, h$ can lead to large frequencies at typical substrate temperatures used in magnetic film processing ($\sim 1 \times 10^{13}$ Hz at 480 K).

This simple model for surface diffusion illustrates the role that E_s and especially T can play in altering surface diffusion. The ability to establish thermal substrate conditions promoting or suppressing surface diffusion before the onset of reevaporation is one of the important parameters that can be controlled for magnetic film growth. Another parameter, the surface diffusion length Λ, is useful for understanding thin film growth. In our simple model, it is given by

$$\Lambda = a\sqrt{k_s t} = 2\sqrt{Dt} \qquad (2)$$

where a is the distance between lattice sites, and D is the diffusivity, which obeys an Arrhenius formula:

$$D = D_0 \quad \exp\left(\frac{-E_s}{RT}\right) \qquad (3)$$

As adsorbate atoms/molecules are continuously introduced onto the substrate surface, nucleation is inevitable. The concept of surface energy, which reflects the tendency for molecules in the condensed phase

to feel an attraction to each other, is useful for understanding nucleation. Surface tension (γ) is typically an anisotropic quantity for crystalline solids, due to preferences in chemical bonding direction, and is dependent on many properties of the exposed surface, including chemical composition, crystallographic orientation, atomic reconstruction, and atomic scale roughness. When γ is multiplied by the surface area (which is affected by morphology), the total surface energy is obtained. That is the quantity that is minimized by surface diffusion.

The surface energies of the substrate and the film material strongly influence nucleation. If the surface diffusion length Λ is less than the surface lattice parameter a, then the surface energy is an insignificant parameter, since the reaction is kinetically limited and the growth is quenched (atoms stick where they land). If the situation is not kinetically limited ($\Lambda \gg a$, it is useful to define γ_s as the surface tension of the substrate free surface, γ_i as the surface tension of the substrate–film interface, and γ_f as the surface tension of the film free surface. In this non-kinetically-limited case, the film spreads along, or *wets*, the substrate if

$$\gamma_f + \gamma_i < \gamma_s \tag{4}$$

resulting in a layer-by-layer, or Frank–van der Merwe (FM), growth mode. This mode occurs if there is sufficiently strong film–substrate bonding to reduce γ_i .

If the opposite relation holds for the surface tensions,

$$\gamma_f + \gamma_i \geq \gamma_s \tag{5}$$

spreading the film across the substrate increases the total surface energy, resulting in the drive to lower surface energy by forming three dimensional islands, which is called the Volmer–Weber (*VW*) or island growth mode. A third intermediate growth mode exists, the Stranski–Krastonov (*SK*) mode, in which the islands transition from layer-by-layer growth to VW growth after a couple of monolayers, due to a change in the energy situation (often due to stress reduction) with successive monolayers. These three modes for early film growth are illustrated in Fig. 1, and are especially valuable for understanding the epitaxial growth of magnetic films.

The reduction of γ_i by the use of appropriate seed or buffer layers, or of γ_i and γ_s by energy-enhanced methods (such as ion bombardment), can also be used to promote the FM or layer-by-layer film growth mode. We will discuss examples of this strategy for magnetic films later in this review.

Coalescence of Nuclei and Structure Formation. As mentioned earlier, quenching of surface diffusion can inhibit the formation of nuclei. This is often accomplished by low substrate temperatures during film growth to "freeze out" the nucleation, coupled with the high rate arrival of flux species with insufficient thermal energy for surface diffusion. In this case, the formation of nuclei and their coalescence is kinetically inhibited, and resort to such conditions is sometimes a useful technique for fabricating smooth magnetic films.

If nucleation is not kinetically limited, then various kinetic theories exist that indicate that the density of stable nuclei increases with time up to some maximum or saturation level (N_S) before decreasing. It is predicted that N_S increases with decreasing temperature (or surface diffusion). The stable nuclei decrease in quantity due to coalescence processes. Prior to coalescence, there is a collection of islands of various sizes. In time, the larger islands grow (*Ostwald ripening*) at the expense of the smaller ones, driven by the minimization of surface free energy. Ostwald ripening (27) offers a mechanism for island coalescence that does not require direct island contact, but often does not reach equilibrium during film growth, because the theoretically predicted narrow distribution of crystallite sizes is generally not observed. Additionally, islands in contact can coalesce by sintering (28), while cluster islands migrating across a substrate surface can collide and coalesce by the cluster migration mechanism (27).

Upon the coalescence of nuclei to form a continuous polycrystalline film, various types of film microstructure can develop. This last stage of film growth depends critically on the available adatom mobility available during film growth, which is influenced by the substrate temperature, the vacuum pressure during deposition, and the availability of additional energy enhanced adatom mobilities (commonly found in sputtering). A useful

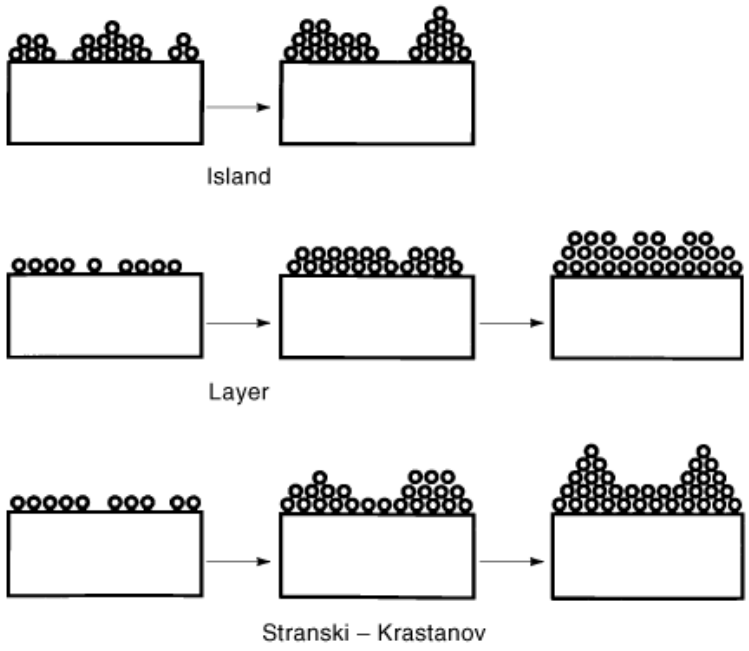

Fig. 1. The three basic film growth modes for early film growth (from Ref. 23). Figure 5-2 (p. 197) of M. Ohring, *The Materials Science of Thin Films,* New York: Academic Press, 1992, Chap. 5.

indicator of adatom mobility is the reduced temperature ($T = T_S/T_m$), the ratio of the substrate temperature to the melting point of the film. Experiments involving evaporated metallic and ceramic films (29) indicated the presence of three structural zones (Z1, Z2, Z3) thoughout the range of the reduced temperature (T), and the presence of a fourth additional transitional zone (ZT) between Z1 and Z2 was observed for sputtered films (30) and other energy-enhanced processes. This is shown for a typical film in cross section in Fig. 2. Based on one study of metallic thin films including ferromagnetic Ni and Co (31), Z1 occurs for $0 < T < 0.1$, ZT for $\approx 0.1 < T < 0.3$, Z2 for $0.3 < T < 0.5$, and Z3 for $T > 0.5$. However, these zones have not been universally identified for all film materials (for example, Z3 is often not observed). Also, it has been observed that the transition between zones is often not abrupt, and is highly dependent on deposition conditions and material. Additionally, this zone growth model does not apply to epitaxial or amorphous films, since they are devoid of high angle grain boundaries. Some materials (e.g., Ti) can undergo anomalous whisker growth, which is the result of an extreme preference for vertical film growth under certain conditions.

There are clear general differences between the four growth zones. For Z1, there is grain renucleation during deposition, with equiaxial grains < 20 nm in diameter, and virtually no grain boundary mobility, due to the extremely low surface diffusion ($\Lambda < a$) . These films consist of columns with poor crystallinity (possibly amorphous) with significant voids. Thicker Z1 films have dome-terminated conelike structures. For ZT, the surface diffusion is still small ($\Lambda < a$) and the growth is still columnar and bimodal in distribution, but the typical use of energy-enhanced processes has removed the voids and dome-terminated cones in the film. For Z2, there is significant surface diffusion, resulting in mobility of grain boundaries. The columns that result in Z2 films have tight grain boundaries and less defective crystallinity, indicative of the onset of granular epitaxy. For Z3, there is considerable bulk annealing of the film during growth, resulting in extensivgrain growth and reduced film porosity. For both Z2 and Z3, the film surface is typically smoother, although surface grain

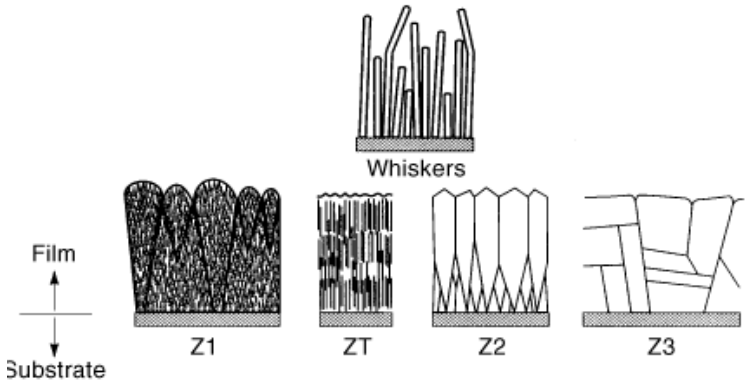

Fig. 2. Characteristics of the four basic structural zones (Z1, ZT, Z2, and Z3) for thick films as viewed through film cross sections. Note that the reduced temperature increases from Z1 to ZT to Z2 to Z3 as described in the text. (From Ref. 24). The upper drawing is an example of anomalous whisker growth. Source: Figure 5.15 (p. 160) of D. L. Smith, *Thin Film Deposition,* New York, NY: McGraw-Hill, 1995, Chap. 5.

boundaries can form grooves. It should be noted that films can evolve from ZT to Z1 or from Z3 to Z2 in certain films as they becomes thicker.

Interfaces. Magnetic films involve interfaces, including those between the film and the substrate, between various film layers, and between the termination of the last film layer and air or vacuum. For magnetic films, the thinner the layers, the greater the fraction of the film that is adjacent to interfaces. This increasing prevalence of interfaces can gives rise to extremely interesting magnetic properties, including interface or surface magnetic anisotropy, which can result in magnetic films with perpendicular magnetic anisotropy. The evidence for surface anisotropy leading to perpendicular anisotropy has been recently reviewed by Shinjo (5) and Gradmann (32) in systems such as fcc Ni(111)/Cu(111), fcc NiFe(111)/Cu(111), fcc Fe(111)/Cu(111), bcc Fe(001)/Ag(001), hep Co(0001)/Au(111), and hep Co(0001)/Pd(111). Shinjo and Gradmann have also reviewed the critical behavior of ultrathin magnetic films.

In many magnetic film structures the interfaces are desired to be smooth and abrupt, but this is seldom the result. The drive to reduce the free energy G, which was earlier de scribed in terms of surface energy minimization, also drives the tendency of magnetic film layers to alloy to some extrnt in proximity of the interface due to the resulting increase in entropy and possible heat of mixing (present in miscible systems like Ni/Cu). The free energy can also be minimized if the materials present at the interface can exothermally react to form intermetallics (common in transition metal silicides and transition metal-rare earth metal systems) or compounds (like transition metal oxides and nitrides). Hence, there is often a competition between the formation of a smooth and abrupt interface between layers with the thermodynamic drive to form interfaces which are defective (diffused, pitted, reacted, or voided). The formation of defective interfaces typically has a significant consequence on the magnetic characteristics of the magnetic thin film.

Generally, the choice of magnetic film deposition process will permit some degree of choice for establishing the structure of the interface. We will examine some examples for magnetic film systems during the upcoming discussion of magnetic film fabrication techniques. Given that surface diffusion is generally faster than the bulk diffusion, it is not surprising that interfacial diffusion processes are often more pronounced while the interface is being established during the deposition process. In view of our discussion of the dependence of surface diffusion length on substrate temperature, it is also not surprising that a reduced substrate temperature (in the Z1 or ZT regime) generally promotes the establishment of more abrupt interfaces and reduces the degree of alloying and intermetallic/compound formation. Interdiffusion is generally much more rapid in polycrystalline

films, due to the presence of grain boundary diffusion, whereas interdiffusion in epitaxial layers is restricted to generally slower interstitial or substitutional mechanisms.

Epitaxial Magnetic Films. The previously discussed concepts of surface energy and surface diffusion are especially critical for the understanding of epitaxial magnetic film growth (see Epitaxial Growth and Magnetic Epitaxial Layers). In addition, the symmetry (crystallographic orientation arrangements) and lattice parameters of the substrate surface in comparison with the intended crystalline structure of the magnetic film cannot be ignored. For example, epitaxial Fe(001)growth on GaAs(001) seems quite plausible given the symmetry between the unreconstructed zinc blende GaAs(001) surface net and the body-centered cubic Fe(001) surface net, coupled with the good fit between the lattice parameter of GaAs ($a_S = 0.5653$ nm) and the Fe lattice parameter ($a_f = 2 \times 0.2866$ nm $= 0.5732$ nm) along the [001] crystallographic direction. The good fit for Fe with GaAs is represented by the lattice misfit parameter f :

$$f = \frac{a_s - a_f}{a_f} = \frac{0.5653 \text{ nm} - 2(0.2866 \text{ nm})}{2(0.2866 \text{ nm})} = -1.38\% \quad (6)$$

In fact, the epitaxial growth of Fe on GaAs has been accomplished (21), but the release of As in the epitaxial Fe film due to FeAs formation typically results in a reduced magnetic moment in thin (<10 nm) iron films. The deposition of an epitaxial ZnSe buffer layer on GaAs can inhibit As diffusion into the epitaxial Fe film. Although low lattice mismatch (<10%) is often an indicator for possible epitaxial film growth, lattice matching is not a sufficient condition for epitaxy. This is obvious when one considers that the 45°-rotated fcc Ag(1) surface net has excellent lattice matching with GaAs ($f \approx 2.3\%$), but that epitaxial growth of Ag(1) on GaAs(1), is impossible without the aid of an Fe or Co seed layer.

Epitaxial films lack high angle grain boundaries, but may have low angle grain boundary defects and twins. Defects from the substrate may propagate into the epitaxial film, and misfit disocations due to lattice mismatches larger than 1% to 2% are also possible. The combination of clean surfaces (which enhance surface diffusion), sufficiently high substrate temperature, and low deposition rate (<0.2 nm/s) generally promotes the surface diffusion conditions for layer-by-layer growth in layers with the proper combination of free substrate, substrate–film (interface), and free film surface tensions.

Amorphous Magnetic Films. Amorphous film materials also have the advantage of avoiding the grain boundaries present during polycrystalline film growth in Z1, ZT, Z2, or even Z3. Because of the strong natural tendency for most materials to form crystals, amorphous magnetic films (metastable metallic glasses) must be fabricated by quenching the crystallization process at low temperatures ($T_S \ll T_m$) as well as the addition of a composition component that does not easily crystallize. It useful to group magnetic amorphous materials in two categories: metal–metalloid (e.g., Fe,Ni,Co + P,B) and early–late transition metal alloys (e.g., NiNb and NiZr). In bulk, amorphous materials are typically quenched from liquid, but amorphous magnetic films are normally quenched from vapor. Amorphous alloys are often formed by eutectic alloys with low T_m (a sign of a suppressed tendency for crystallization). A classic metal–metalloid amorphous magnetic thin film system is $Fe_{70}B_{30}$, a soft magnetic film material with high moment, high resistivity, and low magnetocrystalline anisotropy (33).

Composite Magnetic Films. These films are made by codepositing two or more immiscible materials, which then accumulate into grains of different phases (see Magnetic Particles). Granular Fe films composed of ultrafine Fe particles have been imbedded in amorphous insulating SiO_2 and Al_2O_3 matrices (34) and conductive Cu matrices (35) by sputtering. The single domain nature of these ultrafine Fe particles has yielded materials with greatly enhanced coercivity. More recently, there has been considerable interest in composite metallic magnetic films for granular giant magnetoresistance materials (36, 37) using Ni, Fe, and Co metals and alloys imbedded in immiscible Ag and Cu matrices.

Magnetic Film Fabrication Techniques

When a flux of atoms or molecules arrives on a substrate, they can have energies from ≈0.2 eV to ≈40 eV, depending on the method used for generating the flux. The majority of magnetic films used for research investigations and for magnetic thin film device fabrication are fabricated in vacuum environments by various physical vapor deposition (*PVD*) methods, which can collectively span this wide range of adatom impingement energies. These PVD methods include vacuum evaporation, electron beam deposition, molecular beam epitaxy (*MBE*), various forms of sputtering, and pulsed laser deposition. However, there are also chemical methods of fabricating magnetic thin films, such as electrodeposition, liquid phase epitaxy (*LPE*), and chemical vapor deposition (*CVD*).

In addition, a wide variety of substrate materials are available for fabricating magnetic films. For example, particulate magnetic films for flexible media typically use amorphous organic polymers (typically polyethylene terephthalate or polyester) (38); magnetic films for rigid disk media typically are deposited on polycrystalline aluminum disk substrates (38); single crystalline films for fundamental investigations often are deposited on GaAs (21, 39), Si (40,41,42), sapphire (43,44,45), or MgO (46,47,48,49,50) substrates; and polycrystalline and amorphous films often are deposited on oxided or nitrided Si, Mylar, kapton, quartz, or glass (e.g., Corning glass 7059) substrates.

Electrodeposition of Magnetic Films. The seeds for the resurgence of interest in magnetic film materials in the early 1980s were partly sown by the work of Liebermann et al., who investigated the magnetization of thin polycrystalline films of Fe, Co, and Ni fabricated by electrodeposition (51). Their interpretation of the magnetization of these electrodeposited films as a function of thickness led them to conclude that these magnetic films had "dead" surface layers as a consequence of the reduced dimensionality of the magnetic layers terminating at the interface. It was soon discovered that Liebermann's "dead layer" effect was not a consequence of the fundamental behavior of interfaces, but was rather was an artifact of uncontrolled contamination at the interfaces of the magnetic layer due to the electrodeposition process. Nonetheless, Liebermann's result helped spark vigorous interest in experiments on thin and ultrathin magnetic film in the 1980s to serve as comparisons against the predictions of rapidly improving theoretical models for the electronic structures of magnetic interfaces and magnetic surfaces (5).

Electrodeposition is a simple, economical nonvacuum technique for depositing inorganic films (such as metallic ferromagnetic films) from solution (often aqueous) by electrochemical means (52). The desired metallic film material (such as Ni) is obtained by reduction of its ions at the cathode electrode in an electrochemical cell with the appropriate electrolyte. The source material for the film is the anode, while the film is obtained at the cathode. This process requires the presence of a controlled current input that drives the ion flow (e.g., Ni^{2+} or Co^{2+}) from the anode to the cathode. A classic example for Ni film fabrication is obtained by using a Ni anode (for the source) and a Cu cathode (which serves as a substrate) in a chemical cell containing nickel sulfate and ammonium chloride electrolytes. The ions in the electrolytes used for electrodeposition may be hydrated or complexed, leading to the possibility of contamination of the film by C, N, or O. The modeling of the film formation at the substrate by electrodeposition is typically very complex, far more so than that for vacuum-deposited films. There is also no *in situ* characterization for electrodeposited films.

Liebermann's erroneous results greatly reduced the popularity of electrodeposition for fabricating magnetic films. However, improvements in the electrodeposition technique now permit the fabrication of epitaxial magnetic alloy multilayers (such as Cu/Ni–Co–Cu) from a single electrolyte (53), the fabrication of ultrathin Fe and Co films free of "dead layers" (54), and Co–Ag multilayers and granular films exhibiting giant magnetoresistance (*GMR*) (55, 56). Hence, there may be some utility for this relatively inexpensive technique for fabricating certain metallic magnetic film materials.

High Vacuum Evaporation of Magnetic Films

The fabrication of magnetic films by vacuum evaporation prior to 1965 is nicely summarized in Soohoo's and Prutton's classic texts on magnetic films (25, 26). Due to limitations in vacuum technology, typical ultimate pressures for these vacuum processes were $> 5 \times 10^{-6}$ torr, which led to a worst case contamination accumulation at the film surface of >2 monolayers/s. Simply described, the vacuum evaporation process involves the melting or sublimation of metals in a vacuum, which generates a vapor flux, which is used to form a film at the substrate. Thermal evaporation sources include the twisted wire coil and the dimpled sheet metal boat; the film material coats the wire coil or is placed in the boat. A large current (up to 100 A) at low voltage, is passed through the conductive coil or boat (made of a refractory metal like W, Mo, or Ta) to produce sufficient Joule heating to produce a flux of the desired material.

The high temperatures (typically 1000° to 1500°C) that are required for evaporation can produce significant radiation heating of the nearby substrate, which can lead to uncontrollable adatom mobility at the film surface. In addition, the source material can react or alloy with the coil or boat refractory metal, unless one uses an intervening nonreactive refractory ceramic liner (such as alumina or pyrolytic graphite). The high temperatures can also evolve significant levels of contaminating impurities trapped within the bulk refractory coil or boat material. Flux rates from these sources can fluctuate during film growth, and the distribution of material is lobed ($\cos\theta$ distribution), leading to significant thickness gradients across the film surface. Many refractory materials (such as Mo) cannot be thermally evaporated, and most alloys or compounds either lose stoichiometry or decompose. The adatom energies for evaporated films is low, generally <0.2 eV.

The limitations on the vacuum environment, substrate thermal control, *in situ* characterization, and material purities greatly hampered progress towards magnetic film fabrication until the 1980s. In recent times, high vacuum thermal evaporation has lost its popularity, but it has led to more refined high vacuum and ultrahigh vacuum deposition processes, which produce magnetic films with higher quality and better control.

Electron-Beam-Evaporated Magnetic Films. The high vacuum thermal evaporation technique previously described has evolved into other, more sophisticated high vacuum and ultrahigh vacuum deposition techniques. One evolutionary product is the electron beam evaporation source technique for magnetic film fabrication. Electron beam evaporation sources rely on high energy electron bombardment to vaporize source materials. The electron beam (~1 A current is common) is thermionically generated from a hot W filament, and is magnetically steered and electrostatically accelerated (~10 kV potential typical) towards the source material, which is typically held at ground potential (57).

The basic schematic for an electron beam source is shown in Fig. 3. The intense energy (~10 kW) delivered by the impacting electron beam locally evaporates the source material without excessive heating of the crucible. The crucible is typically made of pyrolytic graphite, tungsten, molybdenum, or platinum in good thermal contact with a water-cooled copper hearth.

Electron beam evaporation extends to refractory metals that are not amenable to thermal evaporation techniques. Also, the reduced heat load to the crucible and water-cooled copper hearth minimizes the thermal outgassing of contaminants encountered in thermal evaporation. As with thermal evaporation sources, the typical adatom arrival energy from an e-beam source is <0.2 eV. Disadvantages of e-beam evaporation include a more collimated lobe for evaporant material distribution ($\cos^n\theta$ pattern, where $n = 2$ to 4, instead of $n \approx 1$ for thermal evaporation sources), which can be widened with the use of a rastering electron beam; a more variable deposition rate, requiring a feedback loop with a film thickness monitor; possible damage to the film by the soft X rays generated by the electron beam impingement onto the source; and the possibility of enhanced macroparticle spitting, leading to defects in the magnetic film. If a reactive gas (such as oxygen) is introduced into a deposition system using e-beam sources, compound films can be formed thanks to the partial dissociation and ionization of the reactive species with the intense electron beam.

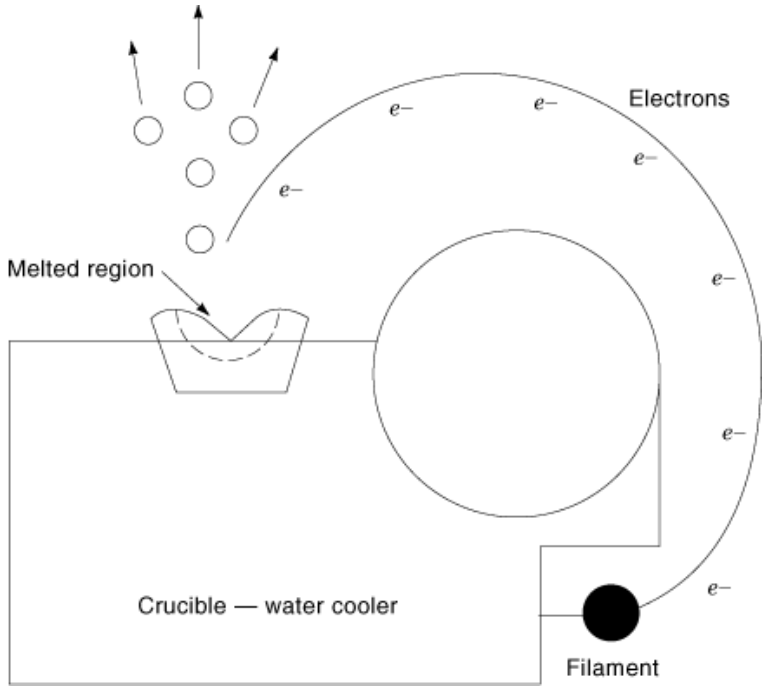

Fig. 3. The schematic for a basic electron beam evaporation source. The crucible contains the solid source material that is intended for deposition. The electron beam is steered by the Lorentz force from the tungsten filament towards the crucible material by the presence of a perpendicular magnetic field generated by a permanent magnet (not shown).

A wide variety of magnetic films have been fabricated using e-beam deposition methods. For example, Chaiken et al. used high vacuum e-beam deposition to fabricate uncoupled Fe–Cu–Co sandwiches exhibiting significant GMR characteristics (58). Magneto-optically active polycrystalline FeCo/Pd multilayers (with perpendicular anisotropy) and Co/Pt films were also recently fabricated by e-beam evaporation (59,60,61). Ultrahigh vacuum environments have been coupled with e-beam sources to produce epitaxial films such as fcc Co on Cu (62) and magnetically coupled bcc Fe/Cr(001) sandwiches (63) the construction of compact metal rod feed e-beam sources compatible with ultrahigh vacuum environments has made these compact e-beam sources useful for ultrathin epitaxial magnetic film research (64). In addition, e-beam sources have been used as components in ultrahigh vacuum molecular beam epitaxy (*MBE*) systems to fabricate epitaxial magnetic films. Examples will be discussed in the upcoming MBE section.

Pulsed Laser Deposition of Magnetic Films. A recent alternative to the thermal or electron beam vaporization of magnetic film materials is pulsed laser deposition (PLD). This technique involves the use of an intense narrow-beam pulsed ultraviolet wavelength laser beam (typically from a Nd:YAG or KrF excimer laser) to vaporize the solid source material, and has become increasingly popular for depositing metallic and especially oxide (ferrite) magnetic film materials. This technique has been recently described by Smith (57) and extensively reviewed by Chrisey and Hubler (65). The basic equipment arrangement for a PLD system is shown in Fig. 4.

The microstructure of magnetic films produced by this technique is influenced by the large average kinetic energy of the impinging adatoms (up to 40 eV) and their typically narrow angular distribution, which makes uniform deposition difficult. In addition, PLD films suffer from potential macroparticle spitting from the rapidly thermally shocked target material, which usually leads to structural defects. Typically, PLD systems

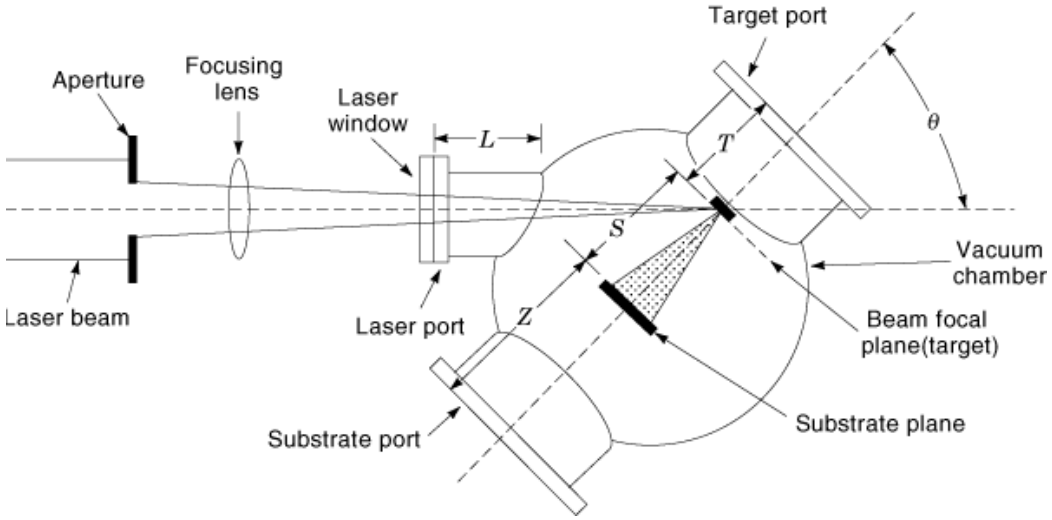

Fig. 4. The basic geometry of a PLD system. The target is made of the source material, and is also the focal plane for the focused laser beam. Important system parameters include the target port to target distance (T), the substrate port flange to substrate distance (Z), the target to substrate distance (S), the laser port length (L), and the angle between the laser beam and the target normal or plume direction (θ). From Chrisey and Hubler, Ref. 65. Source: Figure 2.8 (p. 40) of Chapter 2: Equipment, in D. B. Chrisey and G. K. Hubler (eds.), *Pulsed Laser Deposition of Thin Films,* New York: Wiley, 1994.

are housed in high vacuum base pressure systems (although UHV base pressure systems also exist) and operated at pressures as high as 10^2 Pa. High film deposition rates are possible, although the fine control of film deposition rates useful for creating superlattice structures is difficult. The shallow (tens of nanometers) activated depth of the target source material during the short laser pulse (tens of nanoseconds) encourages the stoichiometric evaporation of multielement materials, and the resulting deposition plume contains a plasma that can activate desired chemical reactions with ionized reactive gases (such as oxygen or nitrogen).

Examples of early PLD fabricated magnetic oxide films include the fabrication of Ni–Zn ferrite films on glass (66) and Bi–YIG films on GGG substrates (67). Development of the PLD process for improved quality magnetic oxide films is represented by work on YIG (68, 69), Bi- and Ga-substituted DyIG films (70), $NiFe_2O_4$ (71), Li–ferrite (72) Co–ferrite (73), and Mn–Zn–ferrite (73). Also, colossal magnetoresistance film materials based on La–Mn–O have been produced by PLD (74,75,76,77,78,79). Metallic magnetic films produced by PLD have been demonstrated for systems such as Co/Pd (80), Fe–Gd–Tb (81), and Fe–Cu (82). For the particular case of Fe–Cu, it has been argued that the much faster deposition made possible by PLD than by thermal evaporation can provide a much greater nucleation density, leading to improved layer-by-layer growth of Fe on Cu(001), overcoming the tendency for roughened Fe film formation on Cu(001) predicted by surface energy considerations (83).

PLD is clearly a promising technique for producing magnetic film materials (especially for rapid prototyping), particularly those involving multielement oxides and nitrides.

Molecular Beam Epitaxy of Magnetic Films. Many would argue that Prinz and Krebs's demonstration of epitaxial Fe films grown on GaAs substrates by molecular beam epitaxy (*MBE*) (84) with excellent magnetic properties helped initiate the modern era of magnetic film research. The MBE technique was pioneered for GaAs film growth (85), and has been reviewed by various authors (86,87,88,89).

The present complexity and relatively high cost of MBE make this technique unpopular for magnetic device manufacturing. However, there are an abundance of examples illustrating the versatility of MBE for

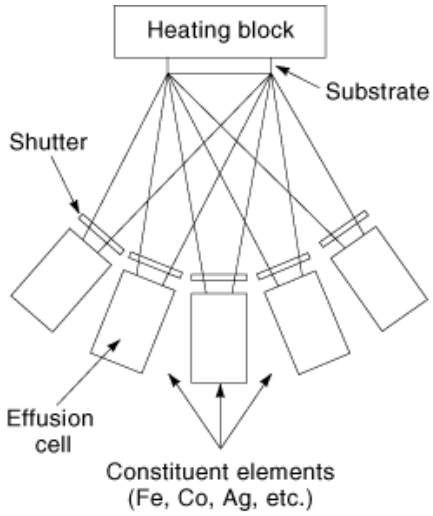

Fig. 5. The basic arrangement of a simple MBE system. The Knudsen cell sources would normally contain magnetic elements like Co or Fe, and nonmagnetic metals like Ag or Cu. The Knudsen sources thermally generate the molecular beam that impinges on the substrate, although e-beam sources are also sometimes used. The typical *in situ* film characterization tools are not shown.

fabricating near-ideal films useful for advancing our understanding of thin film magnetism physics and materials science.

The following factors illustrate the strength of MBE for magnetic film fabrication: (1) the ultrahigh vacuum (UHV $< 10^{-9}$ torr) environment minimizes the opportunity for background contamination, (2) the typical slow deposition rates and low kinetic energies for the impinging atoms (<0.2 eV) enhance the opportunity for controlled kinetic processes promoting epitaxy and metastable crystalline structures, and (3) the UHV environment permits the use of various standard *in situ* surface science characterization methods (reflection high energy electron diffraction, low energy electron diffraction, x-ray photoelectron spectroscopy, Auger electron spectroscopy, scanning tunneling microscopy, etc.), which permit "live time" structural and chemical assessment of the magnetic film. There are also many magnetism-specific analysis techniques that are compatible with the UHV environment in MBE (4), including synchotron techniques such as magnetic circular dichroism spectroscopy (90).

The basic experimental arrangement for the MBE technique is given in Fig. 5, which does not show the additional *in situ* characterization tools typically available for an MBE system. The evaporation source generating the molecular beam is typically a specially designed Knudsen cell source, which is much cleaner, has a wider material angular distribution, and is better controlled than the older thermal evaporation boat or coil. However, electron beam sources are also popular in MBE systems (91,92,93,94), and activated ECR oxygen plasma sources have also been used for fabricating epitaxial Fe_3O_4/NiO films (46).

The ability to promote epitaxy or the formation of metastable structures in single layer or abruptly interfaced multilayers/superlattices has dramatic consequences for properties of magnetic films such as band-structure-dependent crystalline, interfacial, and surface magnetic anisotropy, magnetic moment, micromagnetic characteristics, magnetooptic activity, and spin-polarized electron transport (2,3,4,5,6,7,8,9,10,11,17,21, 32). The ability to fabricate novel phases or epitaxial arrangements of magnetic and nonmagnetic elements in ultrathin form provides theorists with useful quasi-two-dimensional test cases against which tractable *ab initio* theoretical models can be compared (see Magnetic Epitaxial Layers).

In order to produce these near-ideal magnetic film samples, it was crucial to address the materials issues underlying the MBE fabrication of magnetic film materials. For example, Prinz's pioneering demonstration of epitaxial Fe fabrication on GaAs produced films with significant As contamination, whose minimization required the development of an epitaxial buffer layer (ZnSe) on GaAs (95). Prinz's group also found that Fe-seeded layers on GaAs or ZnSe promoted the epitaxial growth of certain noble metal films like Ag, which were useful templates for later epitaxial Fe film growth, and they reported that the use of standard BN crucibles for Fe evaporation yielded a boron film contamination, which Gutierrez et al. (96) later demonstrated was the result of Fe–BN reactivity at elevated temperatures, necessitating the need for alternative refractory ceramic crucible materials such as alumina or beryllia. Analogous substrate preparation techniques were also developed by the magnetism community for single crystal metal substrates [such as Fe whiskers (97)], silicon (91, 92), Nb-seeded sapphire for rare earth superlattices (98), S-passivated Ge (99), and MgO (46, 47, 100, 101).

MBE has been used to stabilize metastable phases such as bcc Co on GaAs (102) and fcc Co on Cu (32, 103). It has also proven to be a useful tool for fabricating films with perpendicular surfaces or interface magnetic anisotropy (32, 93). Furthermore, MBE has proven to be a useful technique for investigating the antiferromagnetic coupling between magnetic layers separated by thin nonmagnetic layers, including epitaxial systems such as Fe–Cr (104,105,106) and Fe–Mo (107), as well as the peculiar 90° magnetic coupling in systems such as epitaxial Fe–Al (108, 109) and CoFe–Mn (110). Unusual single-crystalline magnetic structures can also be stabilized by MBE, including the high magnetic moment $Fe_{16}N_2$ phase (111) on lattice-matched InGaAs substrates, ferromagnetic (Mn,Ni)Al (112) and MnAs (113) epitaxial films on GaAs, epitaxial magnetic rare earth superlattices (43, 99), and ordered crystalline alloys of FePt (94). Molecular beam epitaxy is also an important technique for fabricating magnetic semiconductor films (see Magnetic Semiconductors). In summary, the MBE technique will continue to have an important role in fabricating magnetic films useful for investigating fundamental magnetic phenomena, and may play a future role in developing hybrid ferromagnet–semiconductor (21) or magnetoelectronic applications (11).

Sputtered Magnetic Films. Sputtering techniques are critically important for fabricating research-grade magnetic film structures, and are by far the dominant technique employed for fabricating magnetic film devices. There are several variants of the sputtering technique (see Sputter Deposition and Plasma Deposition), including dc/RF diode sputtering (114,115,116), dc/RF magnetron sputtering (114,115,116,117,118), S-gun sputtering (114), and ion beam sputtering (114, 118, 119). Part of the versatility of these sputtering techniques is that about 51 elements (including all the ferromagnetic elements) and innumerable compounds can be sputter-deposited as films. Also, amorphous, polycrystalline, composite, textured, and epitaxial magnetic films can be sputter-fabricated.

Sputtering is a momentum-transfer technique for eroding materials off a target surface and depositing a portion of the resulting material flux onto a nearby substrate. The target erosion is done with energetic ion impingement (typically Ar^+) from a plasma (also called the glow discharge), and the presence of reactive gases (like oxygen and nitrogen) in the plasma can be used to activate the formation of high-quality oxide compound films (e.g., magnetic oxides and nitrides). The water-cooled target source is generally kept cool enough to effectively eliminate bulk diffusion of alloys and compounds, making sputtering a useful method for fabricating stoichiometric multielement films. The availability of large target sources permits uniform film distribution over large surfaces. Improvements in the purity of sputtering gas sources and gas delivery systems available from suppliers have essentially eliminated the incorporation of reactive gas impurities in sputtered films despite the high operating pressures required for processing.

Diode-Sputtered Magnetic Films. The simplest and least expensive form of sputtering is the diode arrangement, shown in Fig. 6. Electrically conductive target materials can be dc or *RF* (radio frequency) sputtered, while insulating targets must be *RF*-sputtered. Diode sputtering systems can also have dc/RF electrical biasing at the substrate to promote low energy bombardment of the film surface for film modification. Diode systems typically maintain high vacuum base pressures, and operate between ~10 and ~100 mtorr in order to maintain the needed plasma (glow discharge) for sputtering. The impact of electrons at the substrate is

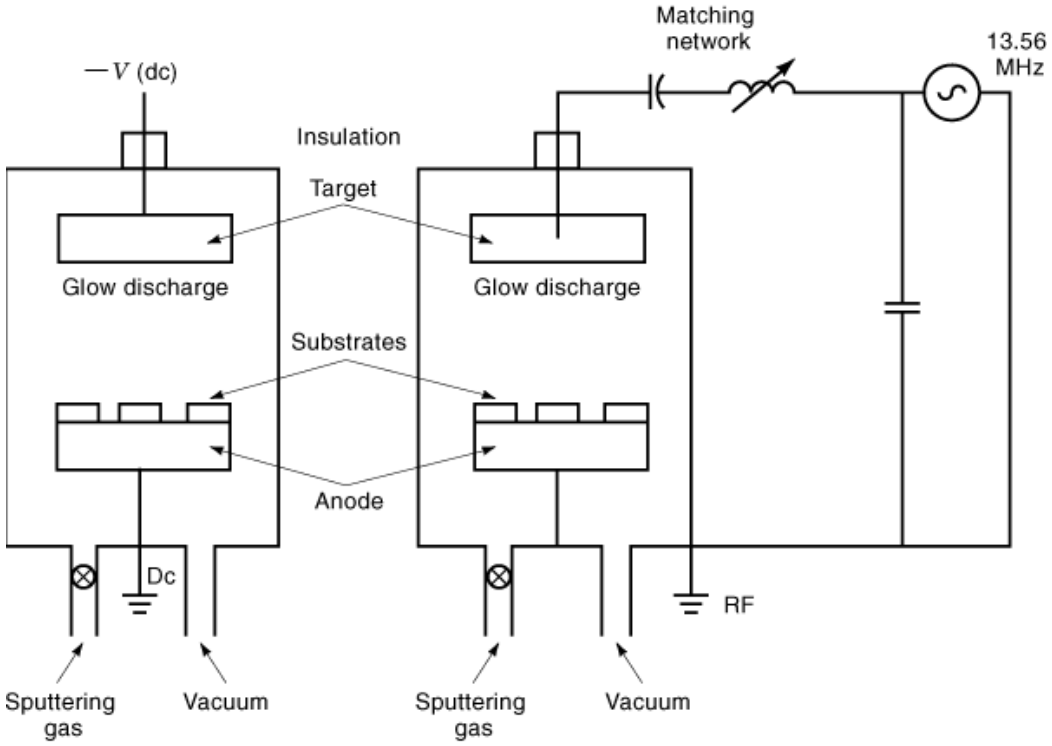

Fig. 6. The basic arrangement of a diode sputtering system, both dc (left) and *RF* (right). Multiple target sources can be used to form complicated film structures, and the bias can often be electrically dc–RF-biased to attract gas ions for low energy bombardment of the film surface during growth. The glow discharge refers to the plasma critical for the sputtering process.

a significant phenomenon, sometimes causing substantial substrate heating that is difficult to control. The high operating pressures for diode sputtering and the resulting shorter mean free path can thermalize the sputtered target flux, resulting in an average depositing atom kinetic energy <0.2 eV (120). The need for high operating pressures and the potential for electron beam bombardment of the substrate has made dc diode sputtering unpopular for magnetic film fabrication. Recent examples of implementation of diode sputtering (typically using the more popular *RF* diode sputtering) include NiCoO-based spin valves (121), CoCrTa longitudinal recording media (122), high-coercivity SmCo films (123), magnetically soft FeAlN films (124), and columnar grain FeN films (125).

Magnetron-Sputtered Magnetic Films. A method for lowering the operating pressure for sputtering and confining the plasma closer to the target and away from the substrate (reducing electron bombardment at the substrate) involves the use of a magnetron sputtering source. The extended lower range of operating pressure for magnetron sputtering than for diode sputtering results in a greater range of impinging atom energy selectivity (from 0.2 eV to a few electron volts per particle) due to reduced thermalization of the sputtered material flux at lower pressures. The most popular magnetron configuration is a planar source, either circular or rectangular. The multipole arrangement of magnets typically produces ≈150 Oe average magnetic field just above the target, helping to confine the plasma to this region via Lorentz forces. For ferromagnetic targets (such as Fe), extremely powerful rare-earth permanent magnets must be used to overcome the shunting effect of the permeable magnetic target. However, the utilization (erosion) of the target is less efficient in magnetron sputtering compared to diode sputtering.

By far, magnetron sputtering is the most popular method for fabricating magnetic thin films. Some representative examples of magnetron-sputtered magnetic films include amorphous Tb–Fe films (126), granular magnetic films (34,35,36,37), Co/Pt multilayers (127), CoNiCr recording media (128), and composite CoPtCr films (129). Magnetron sputtering parameters can be controlled for optimizing the manufacture of magnetic film devices such as magnetic recording heads (12).

Magnetron sputtering systems can be configured for high production automated surveys of magnetic thin film systems, as illustrated by Parkin's survey of >1500 films in investigating the coupling between ferromagnetic layers separated by 3d, 4d, and 5d transition metals (130). It is also possible to place thin interface layers by magnetron sputtering, as in the placement of ultrathin Co layers at the interface of permalloy layers to enhance GMR (131). Magnetron sputtering has been used in many investigations of the effect of thin substrate buffer layers on the microstructure and magnetic properties of film systems such as Cr-buffered CoCrTa (132), Cr- and Ta-buffered permalloy (133), and Ta-buffered NiFe–Cu and CoFe–Cu spin valves (134, 135).

The effect of processing pressure on magnetron-sputtered films has been investigated, since this is an adjustable parameter that has a bearing on the incident adatom energy for film growth. Interesting results include the transition at lower sputtering pressures from a porous Z1 to a denser ZT iron film structure with improved magnetic properties (136), the formation at high sputtering pressures of columnar Co-Cr films with resulting perpendicular magnetic anisotropy (137), and the effect of sputtering pressure on the interface disorder of Fe–Cr multilayers (138). The use of substrate biasing for modifying film microstructure in magnetron-sputtered films has been investigated for magnetic film systems such as Fe–N films (139), NiO pinned spin valves (140), Co/Pt multilayers (141), and CoNiCr films (142). The role of thermal substrate annealing of magnetron-sputtered films has been investigated for numerous magnetic granular materials [(34,35,36,37) and low coercivity discontinuous multilayers (143,144,145) Lastly, magnetron sputtering systems can be used to create epitaxial magnetic film materials such as metastable $Fe_{16}N_2$ (146), soft Fe–FeTa–FeTaN films (147), magnetically coupled Fe–Cr, Co–Cu (148), and Co–Cr (149), and high-coercivity SmCo (150).

Ion-Beam-Sputtered Magnetic Films. A promising alternative sputtering technique for fabricating magnetic films is ion beam sputtering (114, 118, 119). The basic arrangement for a dual ion beam sputtering system is shown in Fig. 7. (see ion beam applications).

Single source ion beam sputtering systems are also available, where the substrate assist source is absent. Likewise, ion-beam-assisted deposition systems where the ion beam assist source is present and the target ion source is replaced by e-beam deposition sources are available. The ion beam is generated by a Kaufman source (115, 151), into which the working sputtering gas is directly injected for plasma generation. The plasma contained in the Kaufman source is extracted and accelerated (typically up to ~2 keV with ~10 eV ion energy spread) via ion optics and used either for sputtering the target or for etching/modifying the substrate (the substrate *assist* process). The Kaufman source permits a greatly reduced chamber operating pressure for ion beam sputtering (~0.1 mtorr) compared to diode or magnetron sputtering, and permits the establishment of independent substrate and target plasma parameters. The lower operating pressures for ion beam sputtering make beam thermalization insignificantallowing for the possibility of high energy target material and reflected neutral fluxes (up to ~10 eV) onto the substrate, which may or may not lead to the formation of high quality magnetic films. Ion beam systems can be configured for either high vacuum or ultrahigh vacuum base pressures.

Examples of single layer magnetic films fabricated by ion beam sputtering and ion-beam-assisted deposition include polycrystalline Ni–Fe films (152,153,154) and Fe and Ni films (155), respectively. In addition, amorphous magnetic films such as TbFe (156) and epitaxial magnetic films such as Fe(1) have been fabricated by ion beam sputtering (157). Ion beam sputtering systems are becoming increasingly popular for the industrial production of thin film magnetic recording heads (158). In addition, ion beam sputtering has proven to be a useful technique for fabricating magnetic multilayers such as Fe/Co (159), Fe/Ag (160), Fe/Al (161), Fe/Mo (162), and Fe/Si (163). The technique has become quite popular for fabricating non-exchange-biased giant magnetoresistance film materials such as NiFe/Cu (164, 165), Co/Cu (166, 167), and CoFe/Cu (168, 169). More recently, ion beam sputtering has been extensively used to fabricate exchange-biased spin-valve

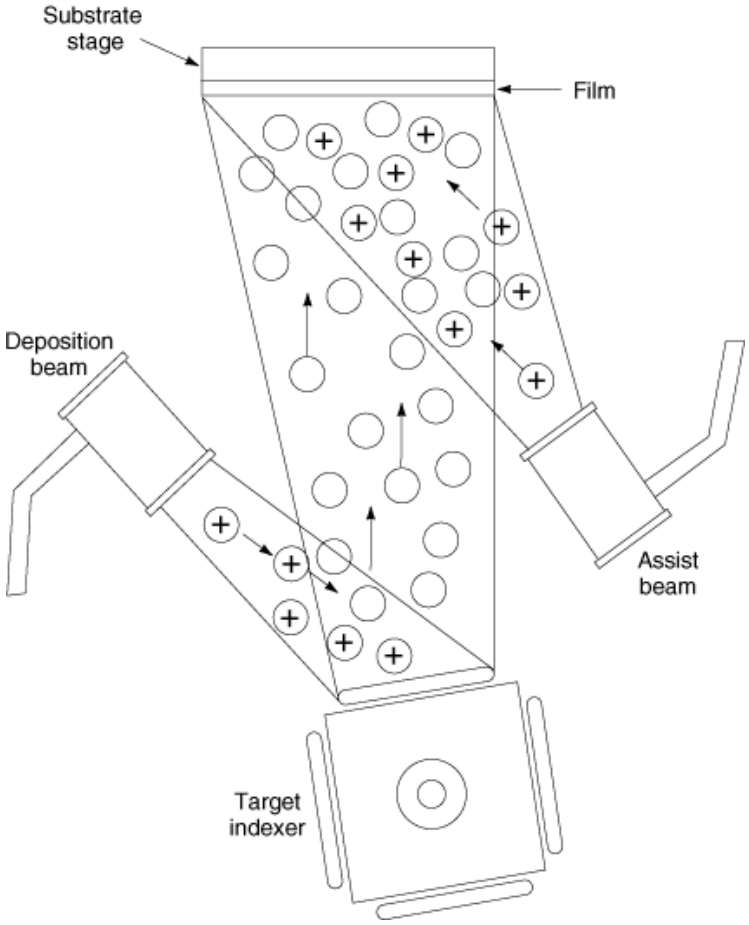

Fig. 7. The basic arrangement for a dual ion beam sputtering system (DIBS). The source of the ion beam is a Kaufman source, from which the ion beam is extracted via grid optics. The *target* ion beam is used for target material sputtering, while the second, *assist* beam is used for etching the substrate or modifying the film during or after growth.

magnetoresistance structures (170,171,172,173,174,175,176). Focused ion beams have also been used to fabricate patterned magnetic multilayers such as Co/Cu (177).

Other Significant Magnetic Film Fabrication Techniques. There are several other film deposition techniques that have found small scale application for fabricating magnetic film materials. One useful technique for ferrite film fabrication is the spin–spray method (178,179,180), which is actually an electroless plating technique. This technique has an extremely low processing temperature that makes it attractive for fabricating polycrystalline ferrite films for nonreciprocal devices, but has suffered from limitations in electrical insulative properties due to the presence of Fe^{2+} ions.

Liquid phase epitaxy of YIG films has been demonstrated (181), and metal–organic chemical vapor deposition (*MOCVD*) (see Chemical Vapor Deposition) has also been demonstrated for Co–Ni–C (182) and NiO films (183). Despite this demonstration, chemical vapor deposition is not the dominant method for magnetic film fabrication (in contrast with silicon semiconductor processing). In the absence of the need for high-aspect-ratio conformal coating in present-day magnetic film devices, the generally lower toxicity of the various PVD processes has been an advantage over MOCVD processes.

Summary and Further Reading

There are many complementary methods for fabricating magnetic films. The continuing development of these techniques will provide researchers and engineers with a variety of choices for fabricating artificially structured magnetic film materials for both research and device objectives. Advances in this rapidly developing field of magnetic films are reported in special issues in the *Journal of Applied Physics* covering the Annual Conferences on Magnetism and Magnetic Materials (most recently contained in Volumes 69, 70, 73, 75, 76, 79, and 81 recently contained in Volumes 69, 70, 73, 75, 76, 79, and 81), special issues in the *IEEE Transactions on Magnetics* covering the annual Intermag Conferences (most recently contained in volumes 27, 29, 30, 31, and 33), select symposia of the Materials Research Society (including Volumes 150, 151, 232, and 384), and the *Journal of Magnetism and Magnetic Materials* (which also includes special issues on various international conferences on magnetic materials and recording such as MML'93 in Volume 126). Within this encyclopedia, related entries include Magnetic Epitaxial Layers, Magnetic Logic, Magnetic Materials, Magnetic Microwave Devices, Magnetic Particles, Magnetic Recording Heads, Magnetic Semiconductors, Magnetic Sensors, Magnetic Storage Media, Magnetic Tapes, Magnetoresistance, and Magnetostrictive Devices.

Acknowledgments

The author wishes to thank the NSF–DMR Career Program (DMR 9502413) for partial support assisting the preparation of this article. In addition, he wishes to thank the help of Mr. Anival Ayala (SWT) for his help in the preparation of some of the artwork for this review.

BIBLIOGRAPHY

1. L. Bruck, *Ann. Phys.*, **26**: 233, 1936.
2. G. A. Prinz, *MRS Bull.*, **13**: 28, June 1988.
3. S. D. Bader, *Proc. IEEE*, **78**: 909, 1990.
4. L. M. Falicov et al., *J. Mater. Res.*, **5**: 1299, 1990.
5. T. Shinjo, *Surface Sci. Rep.*, **12**: 49, 1991.
6. L. M. Falicov, *Thin Solid Films*, **216**: 169, 1992.
7. M. H. Kryder, *Thin Solid Films*, **216**: 174, 1992.
8. R. Wolfe, *Thin Solid Films*, **216**: 184, 1992.
9. A. Barthelemy et al., *Phys. World*, November 1994, p. 34.
10. Special Issue on Ultrahigh-Density Information-Storage Materials, *MRS Bull.*, **21**, September 1996.
11. Special Issue on Magnetoelectronics, *Phys. Today*, **48**, April 1995.
12. S. Gupta et al., *Data Storage*, **2**: 43, 1995.
13. R. E. Fontana, Jr., *IEEE Trans. Magn.*, **31**, 2579, 1995.
14. B. A. Gurney et al., *J. Appl. Phys.*, **81**: 3998, 1997.
15. J. M. Walls (ed.), *Methods of Surface Analysis—Techniques and Applications*, New York: Cambridge Univ. Press, 1989.
16. C. R. Brundle, C. A. Evans, Jr., S. Wilson (eds.), *Encyclopedia of Materials Characterization*, Greenwich, CT: Butterworth-Heinemann, 1992.
17. L. M. Falicov, *Phys. Today*, Oct. 1992, p. 47.
18. R. M. White, *Science*, **229**: 11, 1985.
19. P. Singer, *Semiconductor Int.*, February 1997, p. 71.
20. 1998 Disk/Trend report, Mountain View, CA: Disk/Trend Inc., 1998.
21. G. A. Prinz, *Science*, **250**: 1092, 1990.

22. M. Johnson, *Science*, **260**: 320, 1993.
23. M. Ohring, *The Materials Science of Thin Films*, New York: Academic Press, 1992, Chaps. 5, 7.
24. D. L. Smith, *Thin Film Deposition*, New York: McGraw-Hill, 1995, Chaps. 5, 6.
25. R. F. Soohoo, *Magnetic Thin Films*, New York: Harper and Row, 1965.
26. M. Prutton, *Thin Ferromagnetic Films*, London: Butterworth, 1964.
27. R. W. Vook, *Int. Metals Rev.*, **27**: 209, 1982.
28. R. M. German, *Powder Metallurgy Science*, Princeton, NJ: Metal Powder Industries Federation, 1984.
29. J. A. Thornton, *Ann. Rev. Mater. Sci.*, **7**: 239, 1977.
30. J. A. Thornton, *J. Vac. Sci. Technol.*, **11**: 666, 1974.
31. H. T. G. Hentzel, C. R.M. Grovenor, D. A. Smith, *J. Vac. Sci. Technol.*, **A2**: 218, 1984.
32. U. Gradmann, Magnetism in ultrathin transition metal films, in K. H. J. Buschow (ed.), *Handbook of Magnetic Materials*, Volume 7, New York: North-Holland, 1993.
33. R. J. Hicken et al., *Phys Rev. Lett.*, **64**: 1820, 1990.
34. G. Xiao C. L. Chien, *Appl. Phys. Lett.*, **51**: 1280, 1987.
35. J. R. Childress, C. L. Chien, M. Nathan, *Appl. Phys. Lett.*, **56**: 95, 1990.
36. J. S. Jiang, J. Q. Xiao, C. L. Chien, *Appl. Phys. Lett.*, **61**: 2362, 1992.
37. M. J. Carey et al., *Appl. Phys. Lett.*, **61**: 2935, 1992.
38. E. Koster, Particulate media, in C. D. Mee, E. D. Daniel (eds.), *Magnetic Recording Technology*, 2nd ed., New York: McGraw-Hill, 1996, Chap. 3.
39. E. Schloemann et al., *J. Appl. Phys*, **63**: 3140, 1988.
40. C.-A. Chang, J. C. Liu, J. Angilello, *Appl. Phys. Lett.*, **57**: 2239, 1990.
41. C.-A. Chang, *Phys. Rev. B* **42**: 11946, 1990.
42. F. Giron, P. Boher, *Thin Solid Films*, **226**: 9, 1993.
43. M. B. Salamon et al., *Mat. Res. Soc. Symp. Proc.*, **231**: 95, 1992.
44. B. M. Clemens et al., *J. Mag. Magn. Mat.*, **121**: 37, 1993.
45. J. F. Ankner, et al., *J. Appl. Phys.*, **73**: 6427, 1993.
46. D. M. Lind et al., *Phys. Rev. B*, **45**: 1838, 1992.
47. B. M. Lairson et al., *Appl. Phys. Lett.*, **61**: 1390, 1992.
48. C. Liu, Y. Park, S. D. Bader, *J. Mag. Magn. Mat.*, **111**: L225, 1992.
49. H. Fuke, A. Sawabe, T. Mizoguchi, *Jpn. J. Appl. Phys.*, **32**: L11337, 1993.
50. Th. Muhge et al., *J. Appl. Phys.*, **77**: 1055, 1995.
51. L. N. Liebermann, D. R. Fredkin, H. B. Shore, *Phys. Rev. Lett.*, **22**: 539, 1969; L. N. Liebermann *et al.*, *Phys. Rev. Lett.*, **25**: 232, 1970.
52. F. A. Lowenheim, Part III-1: Deposition of inorganic films from solution, in J. L. Vossen and W. Kern (eds.), *Thin Film Processes*, 2nd ed., New York: Academic Press, 1978.
53. M. Alper et al., *J. Mag. Magn. Mat.*, **126**: 8, 1993.
54. W. Schindler, O. Schneider, J. Kirschner, *J. Appl. Phys.*, **81**: 3915, 1997.
55. H. Zaman, S. Ikeda, Y. Ueda, *IEEE Trans. Magn.*, **33**: 3517, 1997.
56. M. Alper et al., *J. Appl. Phys.*, **75**: 6543, 1994.
57. D. L. Smith, Energy beams, in *Thin Film Deposition*, New York: McGraw-Hill, 1995, Chap. 8.
58. A. Chaiken et al., *J. Appl. Phys.*, **70**: 5864, 1991.
59. S.-C. Shin, *IEEE Trans. Magn.*, **28**: 2766, 1992.
60. H. Brandle et al., *IEEE Trans. Magn.*, **28**: 2967, 1992.
61. K.-S. Moon, S.-C. Shin, *J. Appl. Phys.*, **79**: 4991, 1996.
62. H. P. Oepen et al., *J. Appl. Phys.*, **73**: 6186, 1993.
63. Y. U. Idzerda et al., *Phys. Rev. B*, **48**: 4144, 1993.
64. B. T. Jonker, *J. Vac. Sci. Tech.*, **A8**: 3883, 1990.
65. D. B. Chrisey, G. K. Hubler (eds.), *Pulsed Laser Deposition of Thin Films*, New York: Wiley, 1994.
66. K. Tanaka et al., *IEEE Transl. J. Mag. Jpn.*, **6**: 1001, 1991.
67. H. Kidoh, A. Morimoto, T. Shimizu, *Appl. Phys. Lett.*, **59**: 237, 1991.
68. C. J. Yang, S. W. Kim, Y. S. Kim, *IEEE Trans. Magn.*, **30**: 4527, 1994.
69. B. M. Simion, G. Thomas, R. Ramesh, *IEEE Trans. Magn.*, **31**: 3242, 1995.

70. M. Duan et al., *IEEE Trans. Magn.*, **31**: 3245, 1995.
71. P. Samarasekara et al., *J. Appl. Phys.*, **79**: 5425, 1996.
72. F. J. Cadieu et al., *J. Appl. Phys.*, **81**: 4801, 1997.
73. Y. Suzuki et al., *J. Appl. Phys.*, **79**: 5923, 1996.
74. M. McCormack et al., *Appl. Phys. Lett.*, **64**: 3045, 1994.
75. R. von Helmolt, J. Wecker, K. Samwer, *J. Appl. Phys.*, **76**: 6925, 1994.
76. H. L. Ju et al., *Appl. Phys. Lett.*, **65**: 2108, 1994.
77. S. Jin et al., *Appl. Phys. Lett.*, **67**: 557, 1995.
78. A. Gupta et al., *Appl. Phys. Lett.*, **67**: 3494, 1995.
79. C. L. Canedy, *J. Appl. Phys.*, **79**: 4546, 1996.
80. M. Enrech et al., *J. Appl. Phys.*, **73**: 6421, 1993.
81. N. Cherief et al., *J. Mag. Magn. Mat.*, **126**: 225, 1991.
82. S. Sundar-Manoharan et al., *Appl. Phys.*, **81**: 3768, 1997.
83. H. Jenniches et al., *Appl. Phys. Lett.*, **69**: 3339, 1996.
84. G. A. Prinz, J. J. Krebs, *Appl. Phys. Lett.*, **39**: 397, 1981.
85. A. Y. Cho, J. R. Arthur, *Prog. Solid State Chem.*, **10**: 157, 1975.
86. E. H. C. Parker (ed.), *The Technology and Physics of Molecular Beam Epitaxy*, New York: Plenum, 1985.
87. L. L. Chang K. Ploog (eds.), *Molecular Beam Epitaxy and Hetrostructures*, NATO ASI Ser. E, No. 87, Dodrecht: Martinus Nijhoff, 1985.
88. M. A. Herman and H. Sitter, *Molecular Beam Epitaxy: Fundamentals and Current Status*, New York: Springer-Verlag, 1989.
89. J. Y. Tsao, *Materials Fundamentals of Molecular Beam Epitaxy*, New York: Academic Press, 1993.
90. J. Stohr R. Nakajima, *IBM J. Res. Develop.*, **42**: 73, 1998.
91. K. Rook et al., *J. Appl. Phys.*, **69**: 5670, 1991.
92. R. A. Lukaszew et al., *J. Appl. Phys.*, **79**: 4787, 1996.
93. C. D. England, B. N. Engel, C. M. Falco, *J. Appl. Phys.*, **69**: 5310, 1991; B. N. Engel, M. H. Widemann, and C. M. Falco, *J. Appl. Phys.*, **75**: 6401, 1994.
94. R. F. C. Farrow et al., *J. Appl. Phys.*, **79**: 5967, 1996.
95. G. A. Prinz et al., *Appl. Phys. Lett.*, **48**: 1756, 1986.
96. C. J. Gutierrez, S. H. Mayer, J. C. Walker, *J. Mag. Magn. Mat.*, **80**: 299, 1989.
97. B. Heinrich et al., *Phys. Rev. B*, **38**: 12879, 1988.
98. J. J. Rhyne R. W. Erwin, Magnetism in artificial metallic superlattices of rare earth metals, in K. H. J. Buschow (ed.), *Handbook of Magnetic Materials*, Volume 8, New York: North-Holland, 1995.
99. G. W. Anderson, P. Ma, P. R. Norton, *J. Appl. Phys.*, **79**: 5641, 1996.
100. Y. Y. Huang, C. Liu, G. P. Felcher, *Phys. Rev. B*, **47**: 183, 1993.
101. Y. Park, E. E. Fullerton, S. D. Bader, *J. Vac. Sci. Technol.*, **A13**: 301, 1995; D. J. Keavney, E. E. Fullerton, and S. D. Bader, *J. Appl. Phys.*, **81**: 795, 1997.
102. G. A. Prinz, *Phys. Rev. Lett.*, **54**: 1051, 1985.
103. C. Liu, E. R. Moog, S. D. Bader, *Phys. Rev. Lett.*, **60**: 2422, 1988.
104. P. Grunberg et al., *Phys. Rev. Lett.*, **57**: 2442, 1986.
105. M. N. Baibich et al., *Phys. Rev. Lett.*, **61**: 2472, 1988.
106. J. Unguris, R. J. Celotta, D. T. Pierce, *Phys. Rev. Lett.*, **67**: 140, 1991.
107. Z. Q. Qiu, J. Pearson, S. D. Bader, *J. Appl. Phys.*, **73**: 5765, 1993.
108. A. Fuss et al., *J. Mag. Magn. Mat.*, **103**: L221, 1992.
109. C. J. Gutierrez et al., *J. Mag. Magn. Mat.*, **116**: L305, 1992; C. J. Gutierrez *et al. J. Appl. Phys.*, **81**: 5352, 1997.
110. M. E. Filipkowski et al., *Phys. Rev. Lett.*, **75**: 1847, 1995; J. J. Krebs *et al. J. Appl. Phys.*, **79**: 4525, 1996.
111. Y. Sugita et al., *J. Appl. Phys.*, **70**: 6977, 1991.
112. T. Sands et al., *J. Appl. Phys.*, **73**: 6399, 1993.
113. M. Tanaka et al., *J. Appl. Phys.*, **76**: 6278, 1994.
114. K. Wasa, S. Hayakawa (eds.), *Handbook of Sputter Deposition Technology*, Park Ridge, NJ: Noyes Publications, 1992.
115. J. L. Vossen, W. Kern (eds.), *Thin Film Processes*, 2nd ed., New York: Academic Press, 1978.

116. R. Parsons, Part II-4: Sputter deposition processes, in J. L. Vossen and W. Kern (eds.), *Thin Film Processes II*, 2nd ed., New York: Academic Press, 1991.
117. M. Ohring, *The Materials Science of Thin Films*, New York: Academic Press, 1992, Chap. 3.
118. D. L. Smith, *Thin Film Deposition*, New York: McGraw-Hill, 1995, Chap. 9.
119. J. J. Cuomo, S. M. Rossnagel, H. R. Kaufman (eds.), *Handbook of Ion Beam Processing Technology*, Park Ridge, NJ: Noyes Publications, 1989.
120. I. K. Schuller, C. M. Falco, *J. Appl. Phys.*, **52**: 5803, 1981.
121. C. L. Lin, J. M. Sivertson, J. H. Judy, *IEEE Trans. Magn.*, **30**: 3834, 1994.
122. L. L. Lee, D. E. Laughlin, D. N. Lambeth, *IEEE Trans. Magn.*, **30**: 3951, 1994.
123. K. Chen et al., *J. Appl. Phys.*, **73**: 5923, 1993.
124. J. A. Bain M. H. Kryder, *IEEE Trans. Magn.*, **31**: 2703, 1995.
125. S. Jo, Y. Choi, S. Ryu, *IEEE Trans. Magn.*, **33**: 3634, 1997.
126. V. G. Harris et al., *J. Appl. Phys.*, **73**: 5785, 1993.
127. D. Weller et al., *IEEE Trans. Magn.*, **28**: 2500, 1992.
128. H.-Chu Tsai, M. S. Miller, A. Eltoukhy, *IEEE Trans. Magn.*, **28**: 3093, 1992.
129. T. Shimizu, Y. Ikeda, S. Takayama, *IEEE Trans. Magn.*, **28**: 3102, 1992.
130. S. S. P. Parkin, *Phys. Rev. Lett.*, **67**: 3598, 1991.
131. S. S. P. Parkin, *Appl. Phys. Lett.*, **61**: 1358, 1992.
132. B. B. Lai, M. Tobise, T. Shinohara, *IEEE Trans. Magn.*, **30**: 3954, 1994.
133. R. Jerome, T. Valet, P. Galtier, *IEEE Trans. Magn.*, **30**: 4878, 1994.
134. M. F. Gillies, J. N. Chapman, J. C. S. Kools, *J. Appl. Phys.*, **78**: 5554, 1995.
135. S. Gangopadhyay et al., *IEEE Trans. Magn.*, **31**: 3933, 1995.
136. Y. K. Kim, M. Oliveria, *J. Appl. Phys.*, **74**: 1233, 1993.
137. N. Honda et al., *IEEE Trans. Magn.*, **30**: 4023, 1994.
138. M. J. Pechan et al., *J. Appl. Phys.*, **75**: 6178, 1995.
139. C. Gao, W. D. Doyle, M. Shamsuzzoha, *J. Appl. Phys.*, **73**: 6579, 1993.
140. S. Li et al., *IEEE Trans. Magn.*, **34**: 3772, 1998.
141. S. Honda et al., *IEEE Trans. Magn.*, **28**: 2677, 1992.
142. Y. Deng, D. N. Lambeth, D. E. Laughlin, *IEEE Trans. Magn.*, **28**: 3096, 1992.
143. M. A. Parker et al., *J. Appl. Phys.*, **75**: 6382, 1994.
144. J. D. Jarratt, J. A. Barnard, *J. Appl. Phys.*, **79**: 5605, 1996.
145. M. J. Sablik, *Mat. Sci. Lett.* **15**: 1145, 1996.
146. M. A. Brewer, K. M. Krishnan, C. Ortiz, *J. Appl. Phys.*, **79**: 5321, 1996.
147. L. Varga, W. D. Doyle, *J. Appl. Phys.*, **79**: 4995, 1996.
148. X. Bian, H. T. Hardner, S. S. P. Parkin, *J. Appl. Phys.*, **79**: 4980, 1996.
149. J. J. Picconatto, M. J. Pechan, E. E. Fullerton, *J. Appl. Phys.*, **81**: 5058, 1997.
150. E. E. Fullerton, *J. Appl. Phys.*, **81**: 5637, 1997.
151. H. R. Kaufman, *J. Vac. Sci. Technol.*, **A4**: 764, 1986; H. R. Kaufman, R. S. Robinson; R. I. Seddon. *J. Vac. Sci. Technol.*, **A5**: 2081, 1987.
152. Y. Nagai, A. Tago, T. Toshima, *J. Vac. Sci. Technol.*, **A5**: 61, 1987.
153. J. Lo et al., *J. Appl. Phys.*, **61**: 3520, 1987.
154. R. Selestino et al., *J. Appl. Phys.*, **81**: 5304, 1997.
155. W. A. Lewis et al., *J. Appl. Phys.*, **75**: 5644, 1994.
156. V. G. Harris et al., *IEEE Trans. Magn.*, **28**: 2958, 1992.
157. E. Schloemann et al., *J. Appl. Phys.*, **63**: 3140, 1988.
158. M. Tan, *Data Storage*, **3**: 35, 1996.
159. M. Senda, Y. Nagai, *Appl. Phys. Lett.*, **52**: 672, 1988.
160. S. B. Qadri et al., *J. Vac. Sci. Technol.* **A9**: 61, 1991.
161. T. Hamaguchi et al., *J. Appl. Phys.*, **73**: 6444, 1993.
162. F. Z. Cui et al., *J. Phys. D Appl. Phys.*, **27**: 2246, 1994.
163. A. Chaiken, R. P. Michel, C. T. Wang, *J. Appl. Phys.*, **79**: 4773, 1996.
164. T. Dei et al., *J. Mag. Magn. Mat.*, **126**: 489, 1993.

165. Y. Miyamoto et al., *IEEE Trans. Magn.*, **32**: 4719, 1996; Y. Miyamoto *et al. IEEE Trans. Magn.*, **33**: 3523, 1997.
166. N. Kataoka, K. Saito, H. Fujimori, *J. Mag. Magn. Mat.*, **121**: 383, 1993.
167. S. Schmeusser, G. Rupp, A. Hubert, *J. Mag. Magn. Mat.*, **166**: 267, 1997.
168. N. Kataoka, K. Saito, H. Fujimori, *J. Mag. Magn. Mat.*, **126**: 508, 1993.
169. K. Inomata, Y. Saito, R. J. Highmore, *J. Mag. Magn. Mat.*, **137**: 257, 1994.
170. P. Bayle-Guillemaud et al., *IEEE Trans. Magn.*, **32**: 4627, 1996.
171. R. P. Michel et al., *IEEE Trans. Magn.*, **32**: 4651, 1996.
172. G. Wang et al., *IEEE Trans. Magn.*, **32**: 4660, 1996.
173. Y. Miyamoto et al., *IEEE Trans. Magn.*, **32**: 4672, 1996.
174. S. X. Wang, W. E. Bailey, C. Surgers, *IEEE Trans. Magn.*, **33**: 2369, 1997; D. Guarisco, E. Kay, S. X. Wang. *IEEE Trans. Magn.*, **33**: 3595, 1997.
175. L. Tang, D. E. Laughlin, S. Gangopadhyay, *J. Appl. Phys.*, **81**: 4906, 1997.
176. R. Nakatani et al., *IEEE Trans. Magn.*, **33**: 3682, 1997.
177. S. Nagamachi et al., *J. Appl. Phys.*, **80**: 4217, 1996.
178. Q. Zhang et al., *J. Appl. Phys.*, **73**: 6284, 1993.
179. P. Lubitz et al., *IEEE Trans. Magn.*, **30**: 4539, 1994.
180. C. M. Williams et al., *IEEE Trans. Magn.*, **30**: 4896, 1994.
181. J. D. Adams et al., *J. Mag. Magn. Mat.*, **83**: 419, 1990.
182. Y.-G. Kim et al., *J. Appl. Phys.*, **70**: 6062, 1991.
183. C.-H. Lai et al., *J. Appl. Phys.*, **79**: 6389, 1996.

CARLOS J. GUTIERREZ
Southwest Texas State University